The Design of a Controller for the Steer-by-Wire System*

Se-Wook OH**, Ho-Chol CHAE***, Seok-Chan YUN** and Chang-Soo HAN****

Drive-by-Wire (DBW) technologies improve conventional vehicle performance and a Steer-by-Wire (SBW) system is one of the DBW technologies. The control algorithm of the SBW system was designed in this paper. To verify the control algorithm, the SBW system is modeled using the bond graph method. The first aim of the control algorithm is controlling the steering wheel assist motor to make the real vehicle's steering feel and for a vehicle designer to adjust the steering feel as he finds necessary. Therefore, torque map is designed to determine the steering wheel reactive torque. The second aim is controlling the front wheel assist motor to improve vehicle's maneuverability and stability by using understeer and oversteer propensity of a vehicle. Furthermore, high performance control algorithm is proposed in this paper and Active Roll Stability Control (ARSC) method is designed as one of the high performance control algorithm.

Key Words: Steer-by-Wire, Drive-by-Wire, Torque Map, Steering Feel, Active Roll Stability Control

1. Introduction

1.1 Research background and purpose

The Steer-by-Wire (SBW) system is one part of the Drive-by-Wire (DBW) system that the automobile industry will research in future. The new DBW system will replace mechanical and hydraulic systems for steering, braking, suspension, and throttle functions with electronic actuators, controllers, and sensors. The DBW system will improve overall vehicle safety, driving convenience and functionality significantly. Figure 1 shows the concept design of the Delphi's DBW system.

An SBW system is one in which the conventional mechanical linkages between the steering wheel and the front wheel are removed and the system is operated by electronic actuators. The SBW system has many merits compared with a conventional steering system with a mechanical linkage. To begin with, the SBW system can reduce a vehicle's weight by reducing the number of necessary parts which can lead to energy reduction effectiveness. In addition, the danger of a driver being crushed when there is a front-end collision is eliminated as there is no steering column. Finally, the most valuable merit is that it permits automatic steering and vehicle stability control to be free. For this reason, the study of the SBW system has proceeded. Hayama and Nishiazki (2000) proposed the SBW system using direct yaw moment control based on vehicle stability[6]. Czerny et al. (2000) investigated fail-safe logic using 2 micro controllers to compensate for the Electronic Control Unit (ECU) of an SBW system[7]. Segawa et al. (2001) proposed yaw rate and lateral acceleration control for improving vehicle stability[5].

1.2 Research contents

For a conventional vehicle, the driver gets informa-

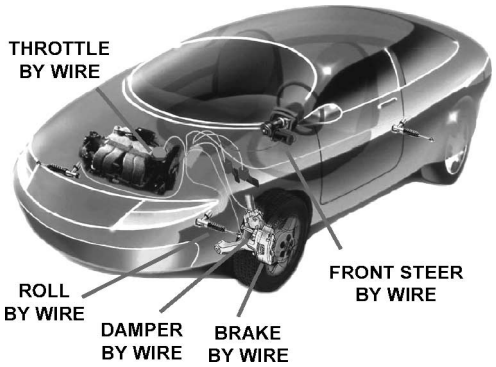

Fig. 1 Drive-by-Wire system

* Received 19th February, 2003 (No. 03-5016)

** Chassis Module R&D Department, HYUNDAI MOBIS, 80–10 Mabook-Ri, Guseong-Eup, Yongin-Shi, Kyeonggi-Do 449–910, Korea. E-mail: ohsw@mobis.co.kr, dolce@mobis.co.kr

*** C&R Lab., Department of Precision Mechanical Engineering, Hanyang University, Sa 1 dong, 1271 Ansan, Kyeonggi-Do 425–791, Korea. E-mail: ikaros72@ihanyang.ac.kr

**** Department of Mechanical Engineering, Hanyang University, E-mail: cshan@hanyang.ac.kr

tion like as a yaw moment by the feedback which is the reaction force generated at front wheel. If steering force feedback is excluded from the SBW system, the feedback information for driving is limited to rolling of the chassis and the driver's feeling of centrifugal force. But it is hard to expect good driving only with the rolling of the chassis and centrifugal force, because resolution of physical body's feeling for centrifugal force and roll effect is lower than that of hand's feeling. For solving this problem, it must be developed to generate the reaction force by using steering motor in the SBW system. This paper discusses a steering wheel motor control algorithm to generate a conventional vehicle's steering feel and to improve driver's steering feel. As a front wheel control algorithm, the vehicle's understeer propensity is used to improve vehicle maneuverability and stability giving the same effect as variable gear ratio between steering wheel and cornering front wheel. To control the front wheel motor, a feed forward control algorithm is employed using the least sensor feedback for low cost control. In addition, a high performance control algorithm is constructed. As one of the control methods, active roll stability is proposed.

Nomenclature

T : Driver's steering torque
$T_{aligning}$: Aligning torque
T_{in} : Initial torque
I_{sw}, I_{sm}, I_{wm}, I_{rb}, I_{tire} : Steering wheel, steering motor, front wheel motor, rack bar, and tire inertia
R_{sw}, R_{sm}, R_{wm}, R_{rb}, R_{tire} : Steering wheel, steering motor, front wheel motor, rack bar, and tire damping
C_{sc}, C_{tr} : Steering column and tie rod stiffness
K_{sm}, K_{wm} : Steering and front wheel motor constant
N_{sm}, N_{wm}, N_{tr} : Gear ratio of steering motor, front wheel motor, and tie rod
i_{sm}, i_{wm} : Motor input current of steering motor and front wheel motor
θ_{sw}, θ_{sm}, θ_{wm}, θ_{tire} : Steering wheel, steering motor, front wheel, and tire angle
$V_{\max}$: Maximum velocity
K_{α} : Angle gain
K_{β} : Velocity gain
e : State error for PID control
k_r : Gear ratio between steering wheel angle and front wheel angle
K : Understeer gradient
a_y : Vehicle's lateral acceleration
δ_f : Front wheel angle
δ_c : Cornering front wheel angle
R : Radius of vehicle cornering
α_f : Front wheel slip angle
α_r : Real wheel slip angle
L : Vehicle wheelbase
V : Forward vehicle speed
t : Vehicle's tread
g : Gravity
K_T : Additional torque gain
K_p : Additional torque proportional gain

2. Steer-by-Wire System Modeling

SBW system modeling used to develop an SBW system controller and a vehicle model applied to the SBW modeling are explained in this chapter. In an SBW system, conventional mechanical linkages between the steering wheel and the front wheel are eliminated and the SBW system is controlled by an ECU through electric wires. Figure 2 shows the overall structure of the SBW system.

The SBW system is divided into two parts a steering wheel and a front wheel and consists of two electronic actuators assisting in their operation. These two electronic actuators receive input signals from an ECU and then one actuator generates reactive torque to the steering wheel and the other actuator steers the front wheel following the driver's will.

2.1 Steering wheel modeling

A steering angle sensor and a torque sensor are located in the steering wheel. The data obtained from these two sensors are transmitted to the ECU and generate output signals to control the steering wheel's reactive torque. The steering wheel, the motor generating reactive torque to the driver and the steering wheel column are modeled using the bond graph method. The reason for using this method is that the steering wheel is composed of mechanical and electric systems. Therefore, the bond graph method easily expresses both the mechanical and the electric systems' energy flow together. Figure 3 shows the bond graph modeling of the steering wheel.

The modeling element of the bond graph consists of the driver's input steering torque, the steering reactive torque motor, and a steering column connecting the steer-

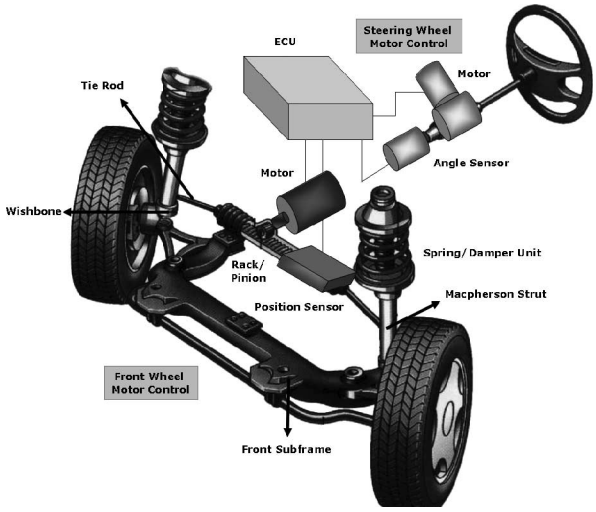

Fig. 2 Steer-by-Wire system

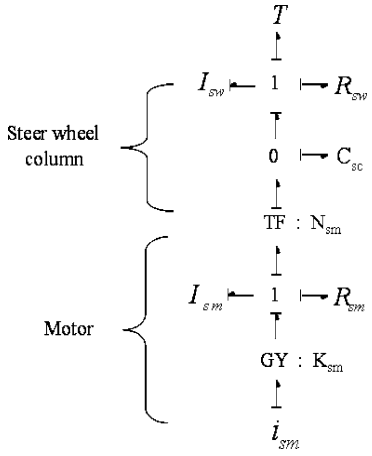

Fig. 3 Bond graph modeling of the steering wheel

ing wheel and the motor. The stiffness of the motor shaft is ignored because it is much smaller than that of the steering column. Following Eqs. (1) and (2) show the equations of the steering wheel modeling.

$$T = I_{sw}\ddot{\theta}_{sw} + R_{sw}\cdot\dot{\theta}_{sw} + C_{sc}(\theta_{sw} - N_{sm}\cdot\theta_{sm}) \quad (1)$$

$$K_{sm}\cdot i_{sm} = I_{sm}\ddot{\theta}_{sm} + R_{sm}\cdot\dot{\theta}_{sm} + N_{sm}\{C_{sc}(N_{sm}\cdot\theta_{sm} - \theta_{sw})\} \quad (2)$$

Equation (1) indicates the driver's torque input and Eq. (2) indicates the steering wheel motor torque input.

2.2 Front wheel modeling

The torque from the front wheel motor is transmitted to the front tires through the front wheel system consisting of a front wheel steering motor, rack & pinion gear, and a tie rod. In addition, there are a rack bar displacement, vehicle velocity and acceleration sensors. The data obtained from it are transmitted to the ECU. The desired steering wheel and front wheel angle can be calculated from a rack bar displacement and vehicle driving conditions. Figure 4 shows the bond graph modeling of the front wheel.

In front wheel modeling, only the tie rod stiffness is considered as it has the greatest effect a vehicle state. Equations (3) and (4) represent the front wheel modeling.

$$i_{wm}\cdot K_{wm} = (I_{wm} + I_{rb}N_{wm}^2)\ddot{\theta}_{wm} + (R_{wm} + R_{rb}N_{wm}^2)\dot{\theta}_{wm} + N_{wm}N_{tr}C_{tr}(N_{wm}N_{tr}\theta_{wm} - \theta_{tire}) \quad (3)$$

$$T_{aligning} = I_{tire}\ddot{\theta}_{tire} + R_{tire}\dot{\theta}_{tire} + C_{tr}(\theta_{tire} - N_{wm}N_{tr}\theta_{wm}) \quad (4)$$

Equation (3) indicates the front wheel motor torque input and Eq. (4) indicates the front wheel aligning torque from the front tire.

2.3 Vehicle modeling

A full-car modeling including state variables for estimating vehicle stability is needed to examine the vehicle's driving properties according to desired control and steering input. Figure 5 shows the full-vehicle dynamics model used in this paper.

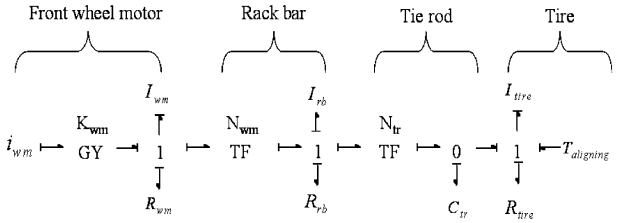

Fig. 4 Bond graph modeling of the front wheel

Table 1 D.O.F. of full-vehicle model

		Parameter	No of Parts	D.O.F
Body		x, y, yaw, roll	1	4
Wheel	Spin	φ	4	4
	Steer	ϕ		1
Total		9 D.O.F		

Table 2 Full vehicle parameters

Parameter	Value	Unit
Vehicle mass, sprung mass	1245 1045	kg
Yaw moment of inertia of vehicle	2014	Kgm2
Dist. From C.G. to front, rear axle	1.29 1.37	m
Front, rear track width	1.42 1.42	M
Front, rear cornering stiffness	38400 31420	N/rad
Tire rolling resistance coefficient	0.012	-
Front, rear roll stiffness	37356 31420	Nm/rad
Front, rear roll damping	1600 1600	Nms/rad
Distance from C.G. to roll axis	0.4	M

In the full-vehicle dynamics model, the important state variables are yaw, roll, x and y-axis direction motion of the vehicle. The Pacejka model is used for the tire model. Table 1 shows the parameters and each D.O.F. used in the full-vehicle model.

In Table 1, pitch direction motion is ignored not because it is related with the vehicle steering performance directly, but because it relates with the acceleration and deceleration performance of the vehicle. Table 2 shows the full vehicle parameters used in the full vehicle model.

Based on these two tables, the established model could be used to study the SBW system. Following Fig. 6 shows the established full-vehicle dynamics model.

2.4 Modeling verification

In this chapter, vehicle modeling and SBW system modeling are verified. To verify the vehicle model, vehicle model simulation results are compared with real vehicle data.

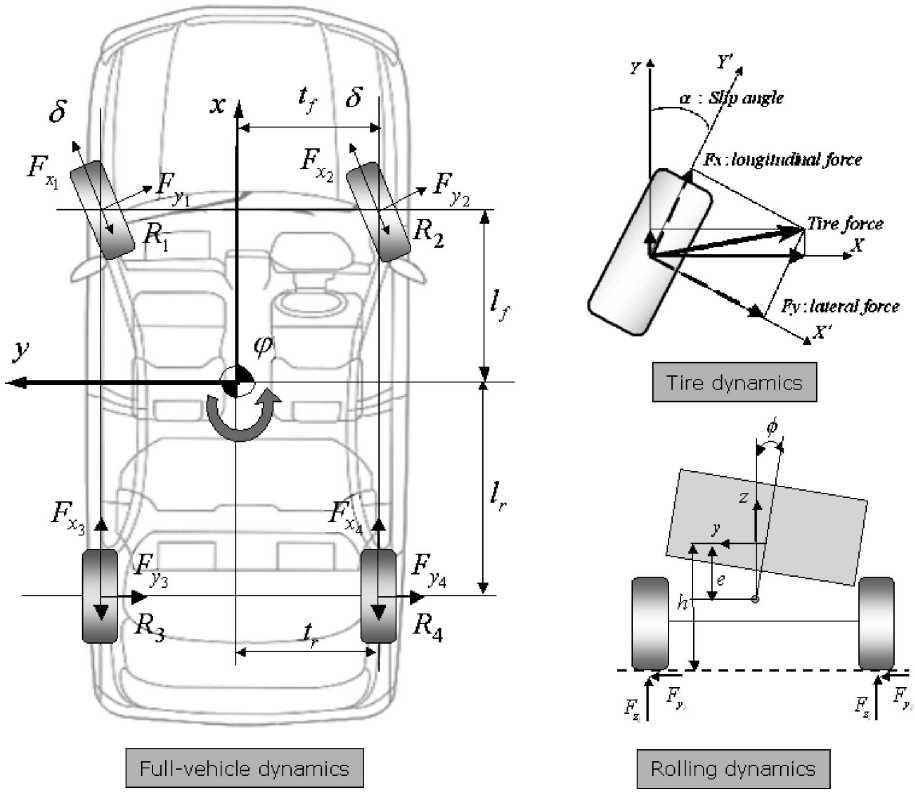

Fig. 5 Full-vehicle dynamics model

2.4.1 Full vehicle model verification In this paper, to verify the full vehicle model, slalom and double lane change tests (ISO3888) are performed. The condition of the above test is the same driver's steering wheel input into the real vehicle and vehicle model at the 80 km/h of vehicle velocity. The steering angle which a driver feeds into the real vehicle is measured by encoder.

The slalom test results of the vehicle steers as shown in Fig. 7. The solid line is the full vehicle simulation results and dashed line is the real vehicle's test results. As shown in Fig. 7, most of the simulation results coincide with real vehicle test results. The little error shown in the figure is probably caused by unmodeled vehicle elements and inaccurate vehicle parameters.

Figure 8 shows the results of the double lane change. The solid line is the full vehicle simulation results and the dashed line is the real vehicle's test results.

As shown in the Fig. 8, most of simulation results coincide with real vehicle test results. Considering the results in Figs. 7 and 8, the full vehicle model is a reliable model that can be used to represent a real vehicle.

2.4.2 SBW system model verification In this chapter, the SBW system model is verified. To verify the SBW system, the SBW system modeling is combined with the verified full vehicle modeling. Therefore, the SBW system modeling could be verified after comparing the simulation results with the conventional full vehicle modeling simulation results. As a test method, the J-turn test is performed and 45°/sec steering angle is inputted at a constant speed of 80 km/h. Figure 9 shows the J-turn simulation results. The late response in Fig. 9 is just properties of SBW system caused by elimination of steering column and addition of control elements.

As shown in Fig. 9, there are negligible differences between the SBW system modeling simulation results and the full vehicle modeling test results. Therefore, it is thought that the SBW system model designed using MATLAB Simulink is proper for representing a real SBW system.

3. SBW System Control Algorithm

The SBW system controller is divided into the steering wheel motor control and the front wheel motor control. The purpose of the steering wheel motor control is to improve the driver's steering feel by generating reactive torque. The purpose of the front wheel motor control is to steer the front wheel angle appropriately for improving the vehicle's maneuverability and stability. Figure 10 shows the rough lay out of general SBW system control algorithm discussed in this chapter.

3.1 Steering wheel motor control

The basic purpose of the steering wheel motor control is to generate reactive torque like a real commercial vehicle when the driver steers. Furthermore, it makes the steering wheel easy to steer at low speeds or when parking the vehicle and to make steering wheel tight at high

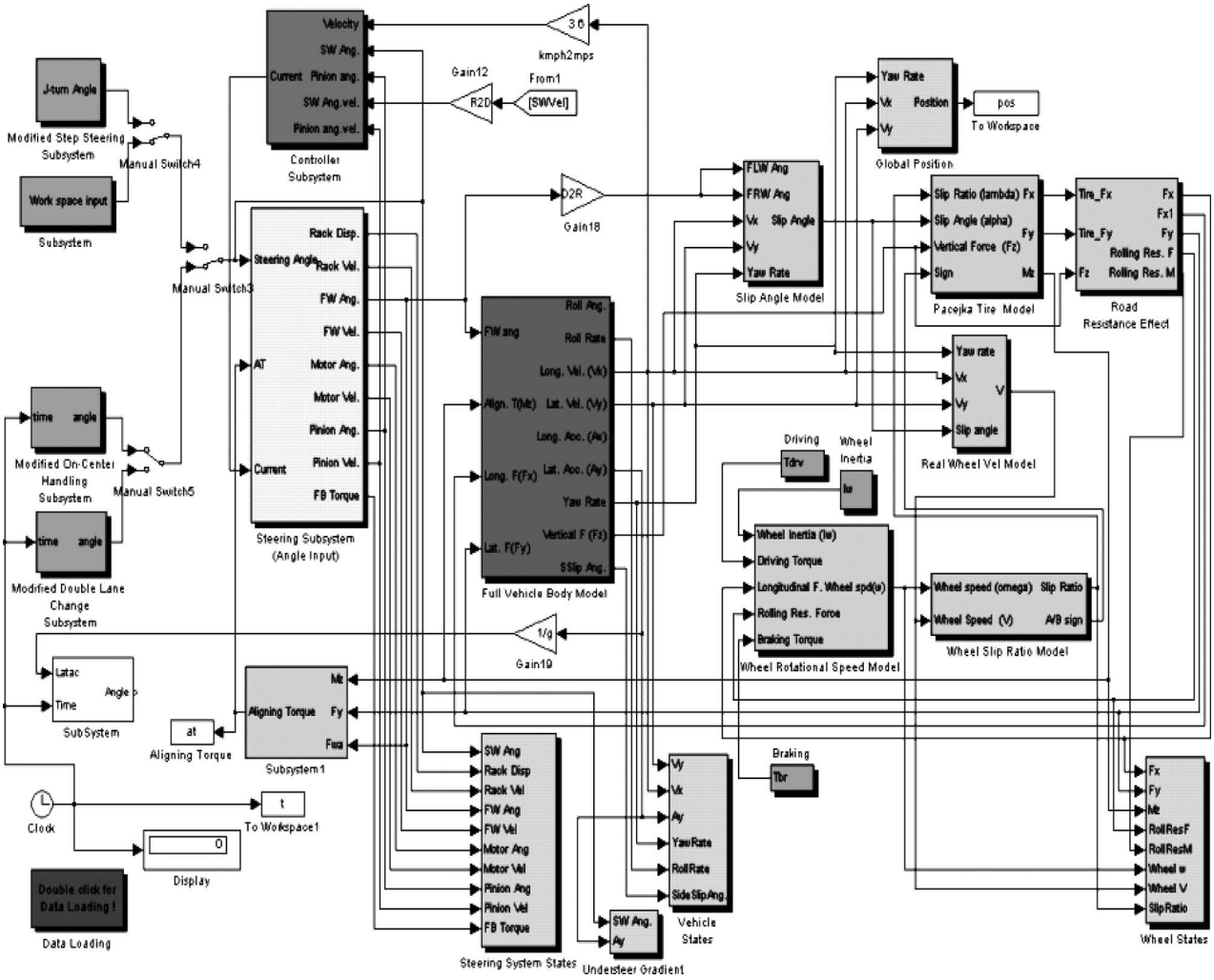

Fig. 6 Full-vehicle dynamics model using MATLAB Simulink

speeds for improving the driver's steering feel by adjusting reactive torque. PID control method is used to control the steering wheel reactive torque motor in this paper. To verify steering wheel motor response, a J-turn angle test is performed.

Figure 11 shows the comparison of the steering wheel motor response between with and without PID control according to the reference steering wheel angle input.

As shown in Fig. 11, even simple PID control satisfies steering response adequately. As a steering wheel control algorithm, control strategy is emphasized in this paper and a torque map is proposed. The reason is that it is impossible to control the steering wheel motor in real time using vehicle dynamics because ECU capacity is insufficient.

As shown in Fig. 12, steering torque is increased according to vehicle speed and steering wheel angle. Steering reactive torque is determined as a function and each parameter for control gain is derived from it. Based on the Fig. 12, the control parameter for the vehicle speed is derived in Eq. (5)

$$y_V = -K_\beta x^2 \left(\frac{1}{3} x - \frac{1}{2} V_{\max} \right) + T_{in} \tag{5}$$

where, x is vehicle velocity, y_V is a component of steering reactive torque corresponding to vehicle velocity, K_β is velocity gain, T_{in} is initial torque, and $V_{\max}$ is maximum speed. Steering torque is determined according to vehicle velocity by using Eq. (5). Therefore, steering reactive torque can be changed according to K_β. Figure 13 shows the steering reactive torque corresponding to vehicle velocity when changing K_β.

As shown in Fig. 13, steering reactive torque is very small at low speeds to make steering easier when parking a vehicle. In addition, steering reactive torque converges at high speeds to prevent excessive torque. With respect to steering wheel angle, Eq. (6) is derived for the control parameter for the steering wheel angle and the square root function is used to present the control concept.

$$y_{SW} = K_\alpha \sqrt{Steering\ wheel\ angle} \tag{6}$$

where, K_α is angle gain, y_{SW} is a component of steering reactive torque corresponding to steering wheel angle. Therefore, steering reactive torque component cor-

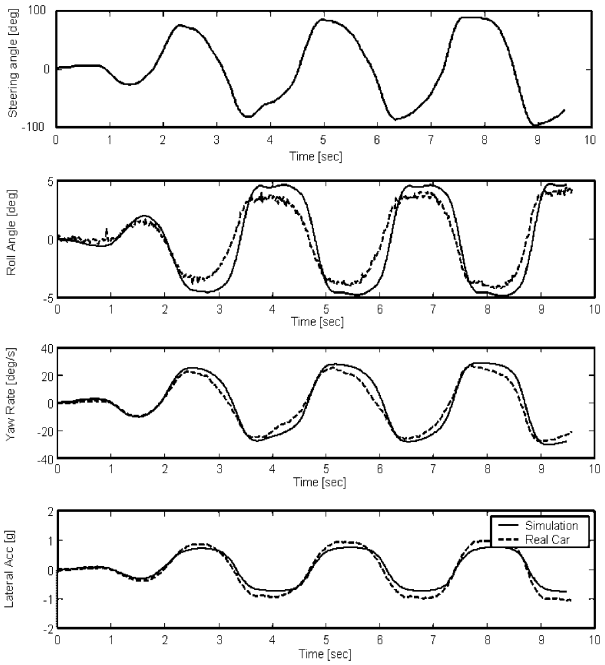

Fig. 7 Slalom test comparison between a real vehicle and a full vehicle model

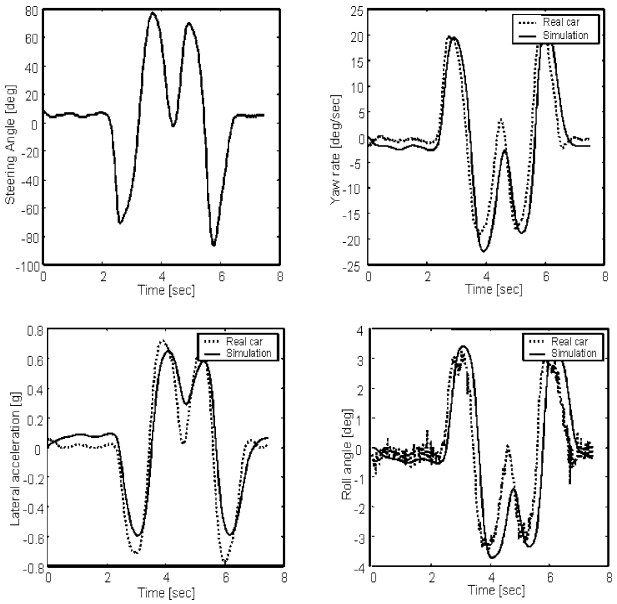

Fig. 8 Double lane change test comparison between the real vehicle and the full vehicle model

responding to steering wheel angle is changed according to K_α, as shown in Fig. 14.

Steering reactive torque is created using two components of steering reactive torque which are related with vehicle velocity and steering wheel angle. In conclusion, steering reactive torque can be determined by changing only two control parameters, K_α and K_β. By adjusting these two control parameters, an overall steering reactive torque map is designed as shown in Fig. 15.

As shown in Fig. 15, at low speeds and parking, steer-

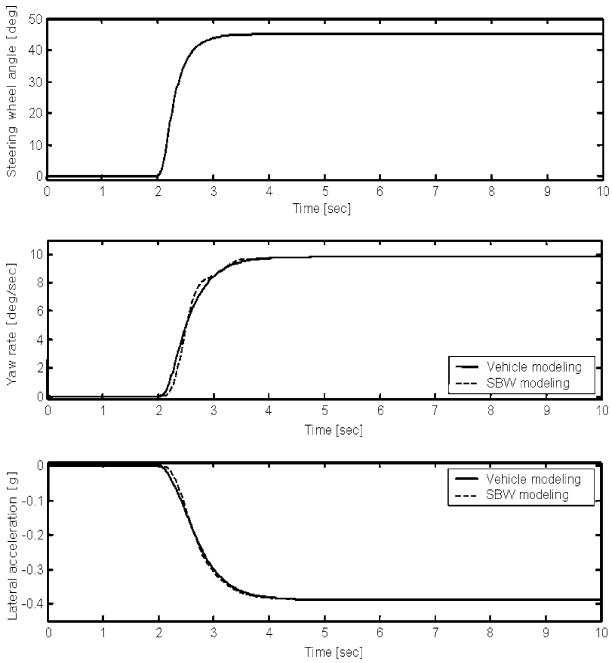

Fig. 9 J-turn test comparison between the full vehicle model and the SBW system model

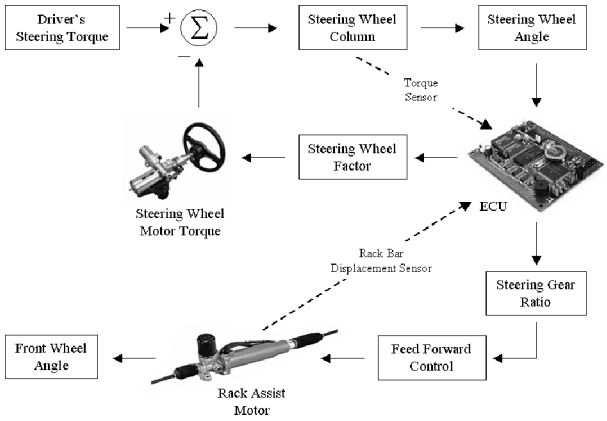

Fig. 10 Overall SBW system control algorithm

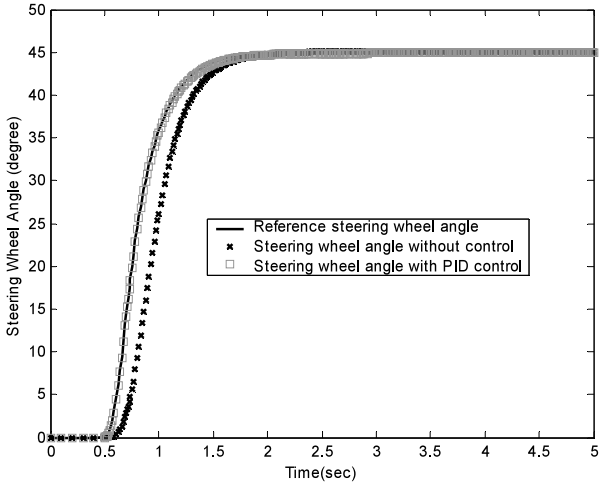

Fig. 11 Steering wheel motor response comparison

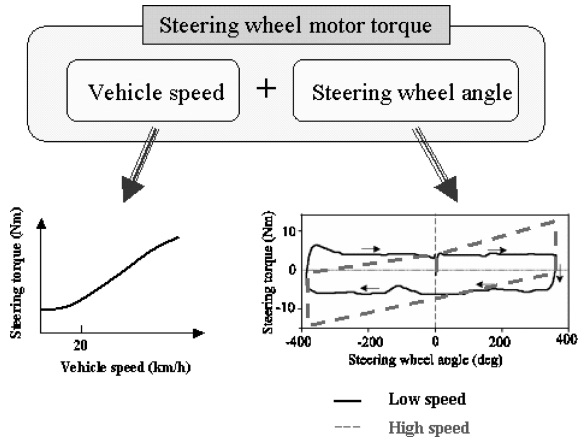

Fig. 12 Steering wheel motor control concept

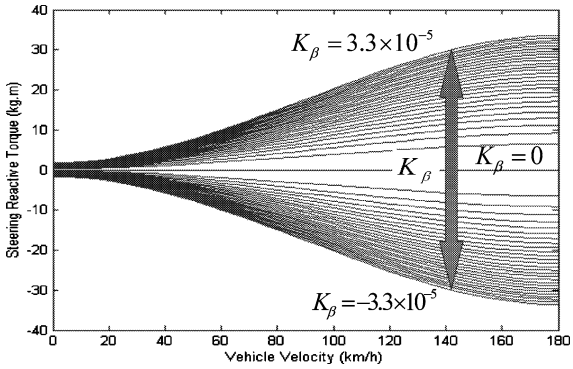

Fig. 13 Steering reactive torque according to vehicle velocity when changing K_β

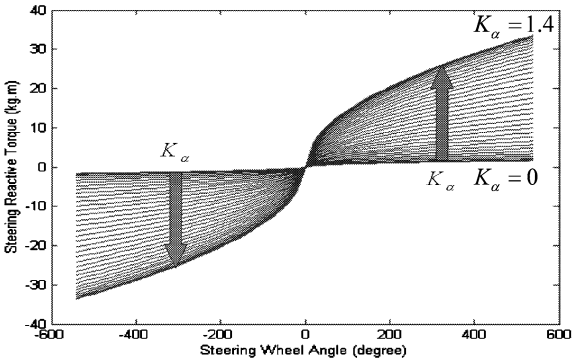

Fig. 14 Steering reactive torque according to steering wheel angle when changing K_α

ing wheel motor torque is kept small and is almost the same with respect to steering wheel angle. However, at high speeds, the steering wheel motor torque is increased according to vehicle velocity and steering wheel angle. As a result, the vehicle designer can control the steering wheel motor torque of the SBW system by using this kind of torque map.

3.2 Front wheel motor control

For control of the front wheels, the ECU outputs front wheel control signals, very important in the SBW system because there is no mechanical linkage between the steering wheel and the front wheel like there is in a conventional steering system.

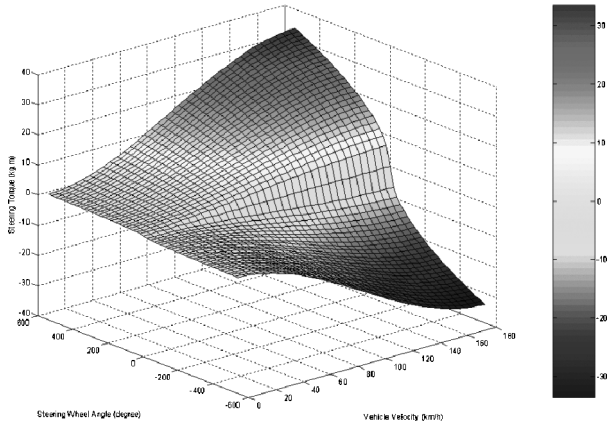

Fig. 15 Torque map for the steering wheel motor control

To control the front wheel motor, the PID control method is used and Eq. (7) is used as state error for PID control.

$$e = k_r\theta_{tire} - \theta_{sw} \tag{7}$$

where, e is state error for PID control, k_r is gear ratio between steering wheel angle and front wheel angle, θ_{sw} is steering wheel angle, and θ_{tire} is front wheel angle.

Front wheel motor control, using the PID control method, as the steering wheel motor control does, compensates front wheel motor performance. Therefore, as a front wheel motor control algorithm, control strategy is emphasized in this paper. The control strategy of the front wheel control is to improve a vehicle's maneuverability and stability. Understeer propensity is controlled for their improvement. Understeer is the front wheels' sideway slip, resulting in a wider line when the vehicle's cornering forces exceed tire performance. Understeer propensity control methods to improve vehicle performance are as follows: Figure 16 shows the control methods as a graphic illustration.

The first method is to improve vehicle maneuverability by driving a vehicle with oversteer propensity. The reason for this is that vehicle's yaw rate and lateral acceleration at a low speed is not important for vehicle stability. On the other hand, with front wheel steering, the vehicle's quick response with respect to the driver's steering is more important for improving vehicle performance. The second method is to prohibit rapid steering, which causes vehicle instability at high speeds by increasing understeer propensity according to increasing vehicle speed. In other words, variable gear effects between steering wheel and cornering front wheel are realized in the SBW system without mechanical linkage. Figure 17 shows a 2 D.O.F bicycle model used for the control methods in this paper.

Equation (8) represents the understeer gradient equation using the bicycle's steady state cornering.

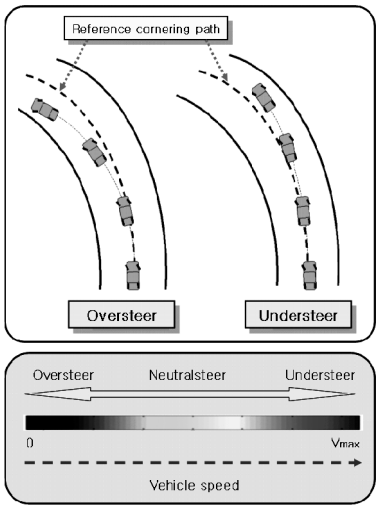

Fig. 16 Understeer propensity control methods

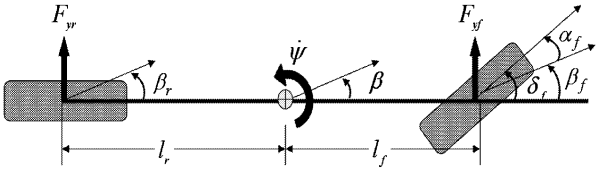

Fig. 17 2 Degree of freedom bicycle model

$$K(\deg/\mathrm{g}) = \frac{1}{a_y}\left(\delta_f - 57.3\frac{L}{R}\right) \tag{8}$$

where,

$K = 0$; *Neutral Steer* $(\alpha_f = \alpha_r)$

$K > 0$; *Understeer* $(\alpha_f > \alpha_r)$

$K < 0$; *Oversteer* $(\alpha_f < \alpha_r)$

In Eq. (8) R is the radius of the vehicle cornering and a_y is the vehicle's lateral acceleration. If R is much greater than the length $(l_f + l_r) = L$ between wheel bases of the vehicle, R becomes $R \cong L/\delta_f$. Here, δ_f is front wheel steer angle. When vehicle lateral acceleration $a_y = V^2/R$ then Eq. (8), the understeer gradient equation, becomes the vehicle cornering angle, Eq. (9)

$$\delta_c = \left(\frac{L}{L + KV^2}\right)\delta_f \tag{9}$$

where,

$$\delta_f = 57.3\frac{L}{R} + K\frac{V^2}{R}$$

$$\delta_c = 57.3\frac{L'}{R}$$

$$R = \frac{L}{\delta_c}$$

From Eq. (9), understeer propensity is increased as vehicle velocity increases because the cornering front wheel angle is reduced as vehicle velocity increases. By using this fact, vehicle maneuverability and stability can be improved at the same time by setting K appropriately according to vehicle velocity, for instance, setting K as a negative number at low speeds or parking for oversteer propensity and setting K as a positive number at high speeds. Therefore, feed forward control would be possible if an appropriate K is selected as a gain parameter of the control algorithm according to the vehicle designer's needs. Figure 18 shows the feed forward control algorithm.

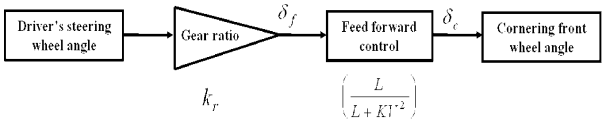

Fig. 18 Feed forward control algorithm

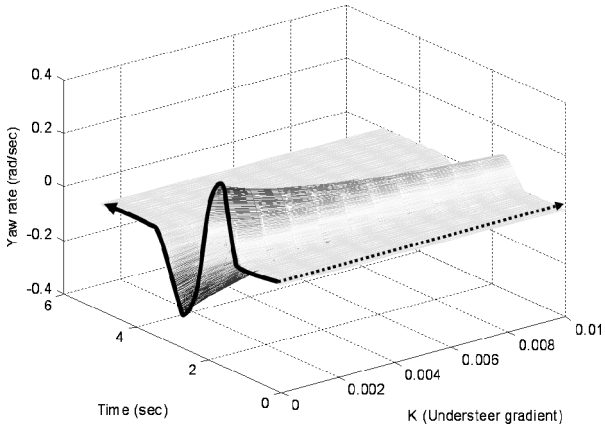

Fig. 19 Lane change simulation with feed forward control for understeer

As shown in Fig. 18, feed forward control does not have to give feedback regarding vehicle states, so lowering costs by not using sensors will be possible. Figure 19 shows the results of lane change simulations with feed forward control describing the yaw rate variation according to changing understeer gradient K from 0 to 0.01 for understeer propensity when vehicle velocity is 80 km/h.

As shown in Fig. 19, vehicle stability can be improved when the understeer gradient is controlled at high speeds because the yaw rate is reduced gradually according to increasing the understeer gradient. Figure 20 shows the results of lane change simulations with feed forward control describing yaw rate variation according to changing the understeer gradient K from 0 to −0.01 for oversteer propensity when the vehicle's velocity is 40 km/h.

As shown in Fig. 20, negative understeer gradient is controlled at low speeds because the yaw rate is increasing gradually as the understeer gradient is decreasing. This improves vehicle maneuverability because the vehicle's quick response for front wheel steering with respect to the driver's steering caused by oversteer propensity improves vehicle maneuverability. By using the understeer gradient control method, vehicle maneuverability and stability control can be improved if the vehicle designer optimizes the understeer gradient as a control parameter according

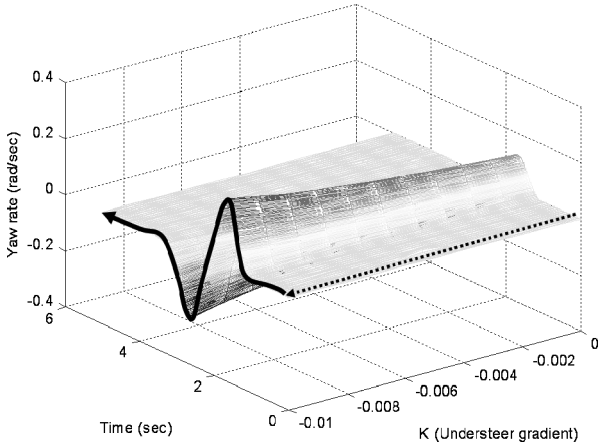

Fig. 20 Lane change simulation with feed forward control for oversteer

to the type of vehicles and drivers.

3.3 High performance control

The high performance control method is a more accurate and advanced control method controlling the front wheel by adding high quality sensors which give exact state feedback to the ECU. The steering wheel reactive torque motor for improving the driver's steering feel is controlled by the desired output through vehicle dynamics after obtaining the vehicle states from a steering wheel torque and vehicle velocity sensor. The front wheel steering motor for improving vehicle maneuverability and stability is also controlled by the desired output through vehicle dynamics after obtaining the vehicle states from yaw rate and lateral acceleration sensors. The control concept of the advanced control method is as follows:

(1) The limits of vehicle instability factors like rollover, yaw moment, and rear sway needs to be set.

(2) When the vehicle exceeds the instability limit, the vehicle dynamics control system operates to decrease vehicle instability factors by controlling motor torque using sensor feedback data.

Figure 21 shows how the high performance control method operates. From the sensor feedback, when the vehicle is about to exceed the instability limit, the vehicle dynamics control unit gives additional reactive torque to the steering wheel, or increases understeer propensity of the front wheel to prevent rollover or yaw moment.

As a part of the high performance control method, the Active Roll Stability Control (ARSC) method is constructed in this paper. To define the rollover threshold, following vehicle rolling dynamics is used. Figure 22 shows the vehicle rolling dynamics.

From this rolling dynamics, the rollover threshold is derived.

$$\frac{a_y}{g} = \frac{t}{2h} \tag{10}$$

By using the rollover threshold, additional torque gain K_T can be determined as follows:

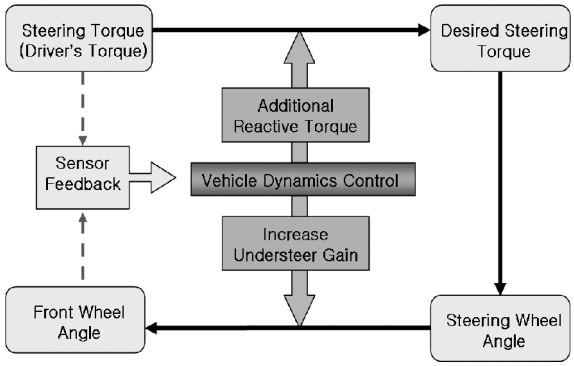

Fig. 21 High performance control method

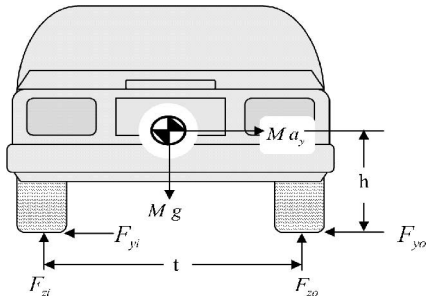

Fig. 22 Vehicle rolling dynamics

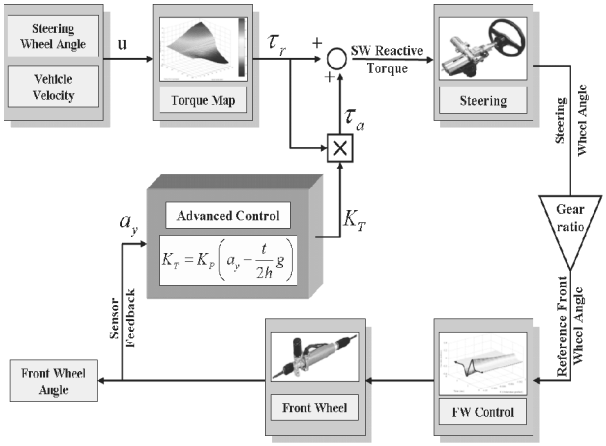

Fig. 23 SBW control algorithm with the ARSC method

$$K_T = K_P\left(a_y - \frac{t}{2h}g\right) \tag{11}$$

where, K_T is additional torque gain, K_P is proportional gain to control K_T and a_y is vehicle lateral acceleration. When vehicle lateral acceleration exceeds rollover threshold, additional torque K_T can be added to prevent rollover. Therefore, all the vehicle designer has to do is to adjust proportional gain K_P to control K_T. Figure 23 shows the overall SBW control algorithm with the ARSC method.

4. Control Algorithm Verification

In this chapter, the SBW system control algorithm proposed in this paper is verified. For verification, the control algorithm computer simulation results are compared with a real vehicle's test results and conventional vehicle

model simulation results.

Figure 24 shows the steering feel response when the torque map algorithm is applied in the SBW system. As shown in Fig. 24, the real steering torque output is almost same as the reference steering torque and its response is fast enough at each speed. Therefore, the steering feel of the SBW system is compared with the real vehicle's steering feel. Figure 25 shows the steering feel comparison results between the SBW system and real vehicle when the vehicle is stopped.

Actually, the steering wheel torque of the SBW system using the torque map algorithm is 3 Nm because the initial torque in the torque map is set to 3 Nm. However, the initial torque is changed to 5 Nm to compare it with the real vehicle and the magnitude of the initial torque can be adjusted in the torque map algorithm. As shown in Fig. 25, the torque map algorithm can compensate the real vehicle's steering feel and it can be adjusted to improve the driver's steering feel.

Another method to evaluate vehicle performance is on-center handling, the region of low lateral acceleration. To improve the vehicle's driving performance in the on-center region, steering torque gradient and steering wheel returnability are very important evaluation factors. Figure 26 shows on-center handling evaluation factors.

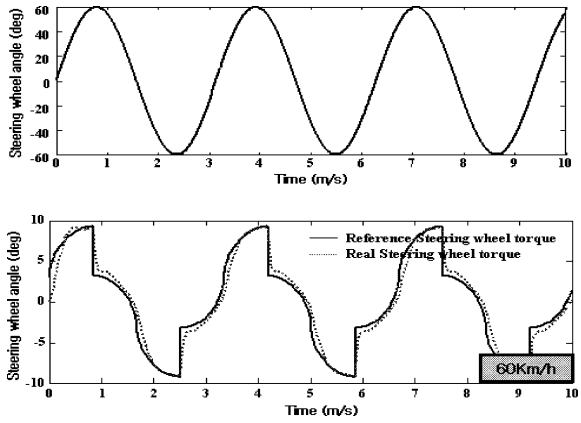

Fig. 24 Steering feel response using torque map

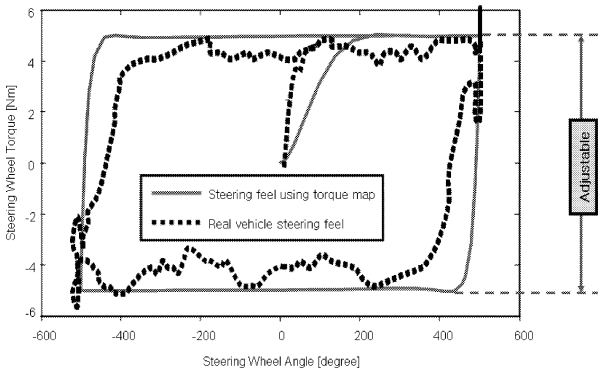

Fig. 25 Steering feel comparison between the SBW system and a real vehicle

Generally, it is thought that on-center handling performance is good when steering torque gradient is large and steering wheel returnability hysteresis is small. Figure 27 shows the comparison between the real vehicle's on-center handling and the SBW system's on-center handling simulation results using the torque map algorithm.

As shown in Fig. 27, returnability hysteresis of the SBW system is much smaller than that of the real vehicle. In addition, the SBW system's steering torque gradient is larger than the real vehicle's. Therefore, it is considered that the SBW system's on-center performance using the torque map algorithm is better than that of the conventional vehicle.

Figure 28 simulation results show the performance of the front wheel control. As mentioned in the front wheel control algorithm, the vehicle's understeer propensity is controlled in this paper to improve the vehicle's maneuverability and stability. The variable gear ratio effect between steering wheel and cornering front wheel is realized by controlling the front wheel motor.

As shown in Fig. 28, the SBW system's yaw rate and lateral acceleration controlled with understeer propensity is lower when compared with the conventional vehicle's computer model. This results show that the SBW system is more understeer and stable in a driving.

Figures 29 and 30 show the slalom test results to verify the ARSC method. For the input steering wheel angle, 60 degree sinusoidal angle is inputted in the test and vehicle speeds are 60 km/h and 80 km/h. Therefore,

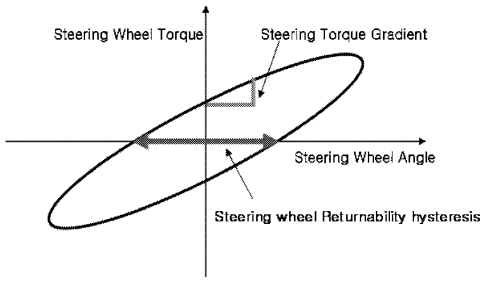

Fig. 26 On-center handling evaluation factors

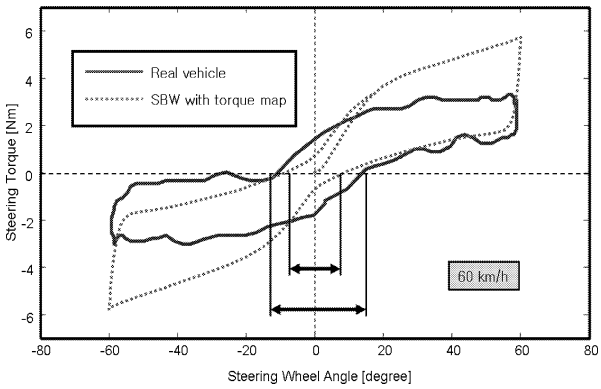

Fig. 27 On-center handling performance comparison

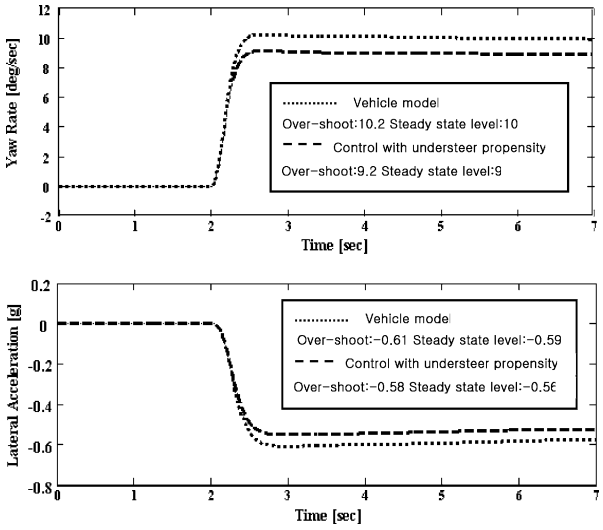

Fig. 28 J-turn angle test

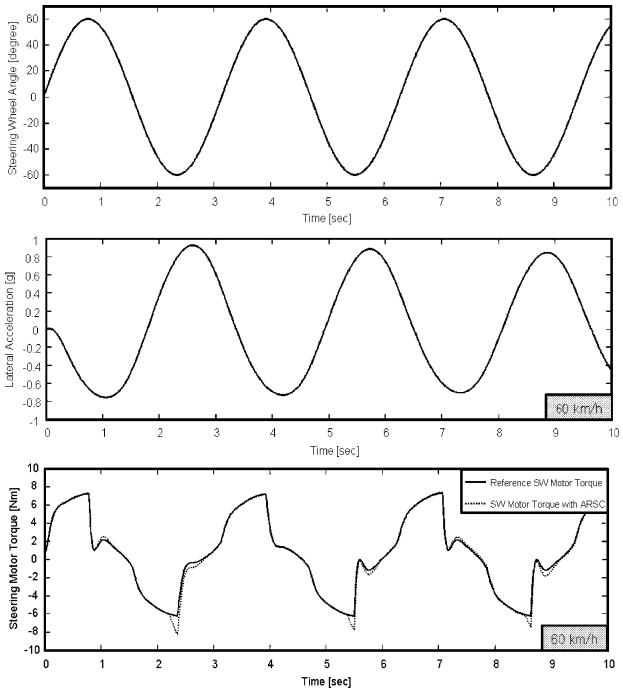

Fig. 29 ARSC method simulation at 60 km/h

the rollover occurrence and how it is compensated using ARSC method can be seen. The conventional vehicle falls into rollover state when their lateral accelerations exceed 0.8 – 1.2 g. It is possible to change this value to the model type of the specific vehicle. The control concept is that when the vehicle's lateral acceleration exceeds the vehicle's instability limit, rollover threshold, additional reactive torque is added to the steering. Therefore, the driver experiences difficulties in steering the vehicle and exceeding the rollover threshold is prevented.

As shown in the simulation results, when vehicle speed is 60 km/h, the lateral acceleration exceeds the instability limit by a very small amount and a little additional

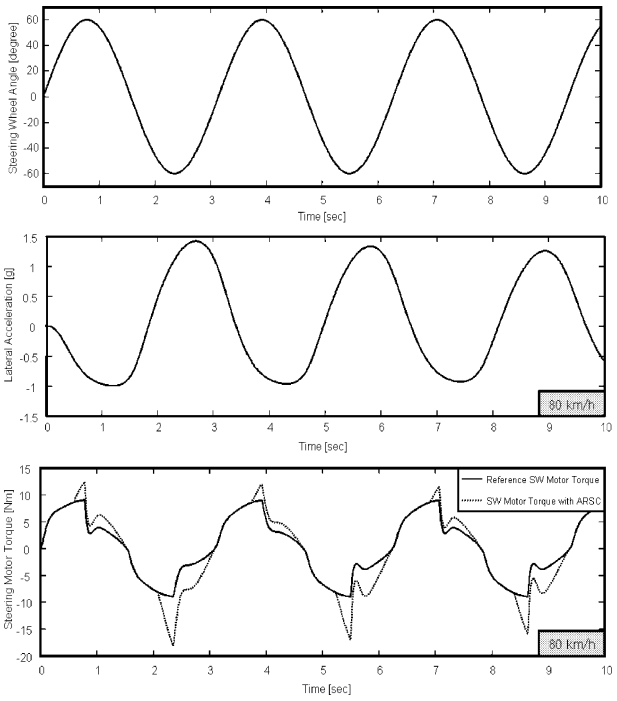

Fig. 30 ARSC method simulation at 80 km/h

torque is added to the steering wheel motor. However, when vehicle speed is 80 km/h, lateral acceleration greatly exceeds the instability limit and then a large amount of additional torque is added to the steering wheel motor. Actually the additional torque proportional gain, K_p, is set to 2 in this simulation. Therefore, the rollover prevention effect can be adjusted by changing K_p. In conclusion, vehicle's rollover could be prevented by using ARSC method.

5. Concluding Remarks

The SBW system's control algorithm was designed in this paper. By using the control algorithm, the SBW system's performance was improved. As a steering wheel control algorithm, the driver's steering feel was improved and the vehicle's maneuverability and stability were improved as a front wheel control algorithm. The concluding details are as follows:

(1) The SBW system was modeled by using the bond graph method and was verified by comparing real vehicle data with a vehicle model.

(2) A steering wheel motor torque map was established to improve driver's steering feel and vehicle speed and the steering wheel angle were used to determine the steering wheel motor torque.

(3) The control parameters to adjust steering feel were derived and the torque map could be controlled easily by using the control parameters.

(4) The understeer propensity control method was used to improve the vehicle's maneuverability and stability and control gain was derived.

(5) Low cost control could be possible using a feed

forward control system using the least number of sensors.

(6) A high performance control algorithm was proposed and ARSC algorithm was designed to prevent the vehicle's rollover.

In conclusion, the SBW system's control algorithm was designed and the performance was verified in this paper. In addition, each control parameter to control the SBW system performance simply was derived and determined in this paper. As future work, the SBW system's fail safe algorithm should be studied.

Acknowledgment

This work has been supported by the Great 7 project (10005145). The author would like to thank Ph. D. Sang-Ho Lee and Un-Koo Lee of research and development division for Hyundai motor company and Kia motors corporation for their assistance.

References

(1) Oh, S.-W., Park, T.-J. and Han, C.-S., The Design of a Controller for the Steer-by-Wire System, FISITA 2002 World Automotive Congress, (2002).

(2) Oh, S.-W., Park, T.-J., Jang, J.-H., Jang, S.-H. and Han, C.-S., Electronic Control Unit for the Steer-by-Wire System Using a Hardware-in-the-Loop-Simulation System, FISITA 2002 World Automotive Congress, (2002).

(3) Park, T.-J., Oh, S.-W., Jang, J.-H. and Han, C.-S., The Design of a Controller for the Steer-by-Wire System Using the Hardware-in-the-Loop-Simulation System, Proceedings of the 2002 SAE Automotive Dynamics Stability Conference, (2002), pp.305–310.

(4) Kim, J.-H. and Song, J.-B., Control Logic for an Electric Power Steering System Using Assist Motor, Mechatronics, (2002).

(5) Segawa, M., Nakano, S., Nishihara, O. and Kumamoto, H., Vehicle Stability Control Strategy for Steer by Wire System, JSAE Review, Vol.22 (2001), pp.383–388.

(6) Hayama, R. and Nishizaki, K., The Vehicle Stability Control Responsibility Improvement Using Steer-by-Wire, Proceedings of the IEEE Intelligent Vehicles Symposium, (2000).

(7) Amberkar, S., D'Ambrosio, J.G., Murray, B.T., Wysocki, J. and Czerny, B.J., A System-Safety Process for by-Wire Automotive Systems, SAE International Congress, Paper 2000-07-1056, (2000).

(8) Park, T.-J., Yun, S.-C. and Han, C.-S., A Development of Hardware-in-the-Loop Simulation System for an Electric Power Steering System, KSME Journal, Vol.24, No.12 (2000), pp.2883–2890.

(9) Segel, L., On the Lateral Stability and Control of the Automobile as Influenced by the Dynamic of the Steering System, ASME 65WA/MD-2, (1998).

(10) Park, T.-J., Yun, S.-C., Han, C.-S., Lee, S.G., Goo, S.S. and Wuh, D.H., The Research on the Lateral Acceleration Control for the MDPS System at High Speed Maneuver, Proceedings of KSAE, (1998).

(11) Boot, R. and Richert, J., Automated Test of ECUs in a Hardware-in-the-Loop Simulation Environment, ASIM 1998 12th Symposium on Simulation Technology, (1998).

(12) Vater, J., The Need for and the Principle of High Resolution Incremental Encoder Interfaces in Rapid Control Prototyping, dSPACE®, (1997).

(13) Jurgen, R., Automotive Electronics Hand Book, (1997), McGraw-Hill.